Check for updates

Dual centrifugation – a novel perspective on lipid nanoparticle formulation development

Valentin Bender, [ID]*† Leon Fuchs,† Monika Köll-Weber, Jan Lembeck,
Laurine Kaul, [ID] Regine Süss and Ulrich Massing

The application of therapeutic RNAs, such as miRNAs, siRNAs, and mRNAs, has emerged as a promising therapeutic approach for treating diseases like cancer. Lipid nanoparticles (LNPs) are widely used for RNA delivery, typically produced using microfluidic mixing systems (MMS). However, MMS manufacturing is rather complex, time-consuming, and cost intensive. Dual centrifugation (DC), an in-vial homogenization technique, offers a straightforward, fast, and efficient alternative for preparing nanoscale lipid formulations, including LNPs. This study focuses on downscaling a DC-based LNP production method to enable 1 mg batch sizes, greatly reducing reagent consumption and allowing high-throughput research. Using a Design-of-Experiment (DoE) approach, key process parameters (lipid concentration, bead amount, and homogenization time) were optimized for small batches of LNPs formulated with cationic or ionizable lipids (DODMA, SM-102, ALC-0315). The optimized process was then applied to produce mRNA- and miRNA-loaded LNPs, which were evaluated for size, size distribution, encapsulation efficiency, and *in vitro* transfection performance. This work introduces DC as a novel and cost-efficient method for producing small-batch size LNPs, with satisfactory size characteristics and *in vitro* performance.

1. Introduction

MicroRNAs (miRNAs) are a class of small non-coding RNAs that regulate gene expression on the post-transcriptional level *via* a process known as RNA interference (RNAi). These small RNAs integrate into the Argonaute-2 protein, forming the RNA-induced silencing complex (RISC), which is crucial for regulating gene expression.[1,2] This process leads to the silencing of target genes, which can be achieved through the mechanisms of mRNA degradation or translational repression.[3,4] The dysregulation of miRNAs has been associated with various diseases, including cancer and neurodegenerative disorders.[5] This has led to the identification of miRNAs as potential therapeutic targets or agents.[6] The field of RNA-based therapeutics has seen significant growth in recent years, particularly during the COVID-19 pandemic. Messenger RNA (mRNA) molecules, the therapeutic ingredient of the mRNA vaccines, have demonstrated the ability to induce the synthesis of therapeutic proteins in cells. This technology is not only being used to develop vaccines but also to treat a range of diseases through targeted protein expression.[7,8]

The delivery of RNA therapeutics faces significant challenges, including poor cellular uptake, endosomal escape, rapid degradation, clearance, and immunogenicity.[4,9] Lipid nanoparticles (LNPs) have emerged as a promising drug delivery system that has shown the potential to overcome these hurdles, as demonstrated by the success of the RNA-based therapeutics like Onpattro® and mRNA COVID-19 vaccines.[7,10] LNPs that contain RNA are typically composed of ionizable lipids, helper lipids, and PEGylated lipids. Ionizable lipids become positively charged at lower pH levels, aiding RNA complexation. These lipids are essential for efficient RNA encapsulation, cellular uptake, and endosomal escape.[11] Helper lipids (*e.g.*, DSPC, DOPE, and cholesterol) influence stability and delivery, while PEGylated lipids have an impact on size, size distribution, and stability.[11]

Today, microfluidic-mixing-systems (MMS) are considered the quasi-standard for the production of RNA-containing LNPs due to their ability to ensure reproducibility, scalability, and the utilization of small batch sizes.[12,13] However, these systems are costly, require labor-intensive solvent removal, and are sensitive to variations in mixing, which in turn affect LNP properties.[14,15] However, virtually all LNP formulations face stability challenges, including aggregation, fusion, as well as RNA and lipid degradation but,[7] due to the complex and time consuming production process, timely preparation prior to administration is not possible.

As an alternative production method, dual centrifugation (DC) has been proven to be suitable. DC enables LNP prepa-

Department of Pharmaceutics, Institute of Pharmaceutical Sciences, University of Freiburg, Sonnenstraße 5, 79104 Freiburg, Germany.
E-mail: valentin.bender@pharmazie.uni-freiburg.de; Tel: +49 761 203-6329
† These authors contributed equally.

ration by in-vial homogenization of a concentrated aqueous lipid/RNA dispersion using ceramic beads as homogenization aid. The homogenization process results in a vesicular phospholipid gel (VPG), which can easily be transferred into a lipid nanoformulation by redispersion (dilution).[16,17] The DC process is based on the concurrent centrifugation of a sample vial around two rotational axes. The rotation around the main rotational axis generates intense centrifugal forces. Concurrent rotation of the vial around the second axis produces frequent changes in the direction of these forces. Due to the horizontal orientation of the vials relative to the second rotational axis, which is at an angle of 40° relative to the main axis in the dual rotor, the in-vial homogenization process leads to high-performance friction as well as a high number of impact events. This results in numerous homogenization events with moderate shear stress, rendering the process both powerful and gentle.[17] With the possibility of preparing 40 samples per run using a modern DC and batch sizes in the lower milligram range, DC is advantageous for formulation screenings.[17–19] Additionally, DC is, in principle, well-suited for the sterile production of lipid nanoformulations prior to clinical administration (bedside preparation), avoiding stability concerns during storage.[17]

Recently, a lipid composition screening for cationic LNPs containing miRNA (miRNA-LNPs) was conducted using DC.[19] The study yielded LNPs with satisfactory size characteristics and excellent knockdown efficiencies for LNPs containing the permanently charged lipid DOTAP, thereby confirming the suitability of DC for LNP preparation. Furthermore, miRNA-LNPs based on the ionizable lipid SM-102 were prepared and the sufficient protonation of SM-102 was achieved without the use of an acidic buffer.[19] Instead, the protonation relied solely on the addition of hydrochloric acid (HCl) during lipid film preparation.[19,20] This resulted in an improved particle size, miRNA encapsulation, and knockdown efficiency.

Despite the encouraging findings, improvements are required for the new DC-based LNP preparation process to ensure a fast and competitive screening approach. This includes reducing reagent consumption, improve LNP size characteristics, and optimizing the acidic conditions for protonation of ionizable lipids. The objective of this study was therefore the downscaling and optimization of the DC-based preparation protocol for miRNA-LNPs with a focus on LNP composition screening, including ionizable lipids. The most critical DC parameters were identified and further optimized for a batch size of 1 mg lipid mixture using a Design-of-Experiment (DoE) approach. Furthermore, the new protocol was applied to conduct a lipid composition screening of miRNA- and mRNA-LNPs using different ionizable lipids.

2. Materials and methods

2.1. Liposomes and LNPs

2.1.1. Materials for liposome/LNP preparation. 1,2-dioleoyl-3-trimethylammonium-propane (DOTAP), 1,2-dioleoyl-*sn-glycero*-3-phosphoethanolamine (DOPE), 1,2-distearoyl-*sn-glycero*-3-phosphocholine (DSPC), and *N*-(carbonyl-methoxy-polyethyleneglycol-2000)-1,2-dimyristoyl-*sn-glycero*-3-phosphoethanolamin (DMPE-PEG2000) were kindly provided by Lipoid GmbH (Ludwigshafen, Germany). 1,2-dimyristoyl-*rac-glycero*-3-methoxypolyethylene-glycol-2000 (DMG-PEG2000) and 1,2-dioleyloxy-3-dimethylaminopropane (DODMA) were purchased from Avanti Polar Lipids (Alabaster, CA, USA), [[(4-hydroxybutyl)azanediyl]di(hexane-6,1-diyl)-bis(2-hexyldecanoate) (ALC-0315) from TargetMol Chemicals Inc. (Boston, MA, USA), cholesterol from Carl Roth GmbH + Co KG (Karlsruhe, Germany), and heptadecan-9-yl 8-((2-hydroxyethyl)[6-oxo-6-(undecyloxy)hexyl]amino)octanoate (SM-102) from DC Chemicals (Shanghai, P.R. China). HPLC gradient-grade ethanol was obtained from Carl Roth GmbH + Co KG. Purified water from an Arium Pro system (Sartorius AG, Göttingen, Germany), 4-(2-hydroxyethyl)piperazine-1-ethanesulfonic acid (HEPES), and sucrose obtained from Carl Roth GmbH + Co KG were used for buffer preparation. Hydrochloric acid (HCl) was purchased from Merck KGaA (Darmstadt, Germany). Custom hsa-miR-100-5p (miRNA) (mature sequence: 5′-AACCCGUAGAUCCGAACUUGUG-3′) was obtained from Horizon Discovery, Ltd (Cambridge, United Kingdom) and CleanCap EGFP-encoding mRNA from TriLink (San Diego, USA).

All materials used were RNase free, sterile, and endotoxin-free. Materials that were not initially sterile or RNase free were heat-treated at 200 °C for 4 hours to eliminate RNase contamination.

2.1.2. In-vial dry lipid film preparation. Lipids were dissolved in ethanol and combined at the desired molar ratios in a 2 mL polypropylene screw-cap vial (Sarstedt AG & Co. KG, Nümbrecht, Germany, Order number: 72.693.005), unless stated otherwise. For formulations containing ionizable lipids, the vials were filled with 400 μL of dissolved lipids in ethanol. Then 10 μL of either 0.1 M, 0.5 M or 1 M HCl was added to achieve the amounts of 1, 5, or 10 μmol of HCl. The vials were vortexed for 5 s prior to vacuum centrifugation using a Concentrator plus (Eppendorf AG, Hamburg, Germany). The final batch size for all experiments was set at 1 mg of total lipid.

For the downscaling and DoE experiments, a molecular-dispersed lipid mixture containing hydrogenated egg phosphatidylcholine and cholesterol (EPC3/Chol) at a ratio of 55 : 45 (mol/mol), was used. This mixture was prepared and provided by Lipoid GmbH. The lipid compositions used for the cationic and ionizable LNPs are shown in Fig. 3 and 4, respectively.

2.1.3. Preparation of liposomes and LNPs

2.1.3.1. EPC3/Chol liposome preparation for downscaling experiments. Liposomes were prepared by DC using a ZentriMix 380 R (Andreas Hettich GmbH & Co. KG, Tuttlingen, Germany). Prior to the DC process, the dry lipid film was rehydrated with an aqueous buffer consisting of 30 mM HEPES and 270 mM sucrose at a pH of 7.4 (SH buffer) to achieve a lipid concentration of 20%, unless otherwise specified. Lipid concentration is defined as the ratio of lipid film mass to total VPG mass (m/m) in the first DC step. Yttrium-stabilized ceramic beads (SiLibeads type ZY-P Pharma, Sigmund Lindner

GmbH, Warmensteinach, Germany) as sizes of either 0.35, 0.9, or 1.5 mm were added as a homogenization aid. The first DC step was performed at 2350 rpm and 4 °C for 5 min. The resulting VPG was redispersed in a ratio of ~1 : 10 (v/v) with SH buffer in the second DC step (1500 rpm, 2 min, and 4 °C). Additionally, different vial sizes, 0.5 mL screw-cap vials (Sarstedt AG & Co. KG, Nümbrecht, Germany, order number: 72.730.406) and 1.5 mL screw-cap vials (Sarstedt AG & Co. KG, Nümbrecht, Germany, order number: 72.703.406) were implemented.

2.1.3.2. EPC3/Chol liposome preparation for DoE experiments. Liposomes were prepared by DC as described above with the following specifications: Vial size and bead size were fixed at 2 mL and 1.5 mm diameter, respectively. The lipid concentration was varied from 10 to 20%, the homogenization time of the first DC step was varied from 3 to 9 min (2350 rpm, 4 °C), and the bead amount was varied from 40 to 140 mg. The tested combinations are listed in Table S1, SI. Confirmation runs were performed with 15% lipid concentration, 7.5 min homogenization time, and 98 mg beads.

2.1.3.3. DoE optimized protocol for cationic miRNA-LNP and empty ionizable LNP preparation. Cationic LNPs (containing DOTAP) were prepared by DC by adding RNase-free H_2O containing 1 mg mL^{-1} micro-RNA-100-5p to the dry lipid film to achieve a lipid concentration of 15%. After adding nine beads with a diameter of 1.5 mm (100 ± 5 mg), the vials were centrifuged at 2350 rpm, for 7.5 min at 4 °C. The resulting VPG was redispersed with SH buffer to achieve a final miRNA concentration of 2.85 μmol L^{-1} in a second DC step (1500 rpm, 2 min, and 4 °C).

For the pH investigation of empty ionizable LNPs dispersions, rehydration and redispersion were performed with deionized water, unless stated otherwise.

2.1.3.4. Preparation of ionizable RNA-LNPs (adjusted DoE optimized protocol). LNPs were prepared by DC according to the following specifications: the dry lipid film was rehydrated with RNAse-free water containing miRNA-100-5p to achieve a lipid concentration of 15%. Different concentrations of miRNA stocks were used to maintain a nitrogen-to-phosphate (N/P) ratio of 6 for all LNPs. The amount and diameter of the beads as well as the DC settings were the same as those used in the optimized protocol (1st DC step 2350 rpm, for 7.5 min at 4 °C and 2nd DC step 1500 rpm, 2 min, and 4 °C). In contrast, 100 μL of deionized purified water was used as the redispersion medium. After the DC process, the dispersion was diluted with 36 μL of a 3.7 times concentrated SH buffer to achieve the same buffer conditions as described before (30 mM HEPES and 270 mM sucrose at pH 7.4). The final miRNA concentration ranged from 4 to 23 μM, depending on the ionizable lipid itself and the molar ratio.

The preparation of mRNA-loaded LNPs followed the same protocol as that used for miRNA-loaded LNPs. However, due to the unavailability of a more concentrated stock solution, a constant mRNA stock concentration of 1 mg mL^{-1} was used in this study. Consequently, the N/P ratio exhibited a proportional increase in accordance with the amount of ionizable lipid used.

2.1.4. DoE approach. The experimental data were statistically analyzed and visualized using Design-Expert® software version 22.0.3 (Stat-Ease, Inc., Minneapolis, MN, USA). A Box-Behnken design was chosen because of its suitability for quadratic-order models. Owing to its near rotatability, this design is appropriate for creating a response to the surface plot and has already been applied in the development of nanoparticles.[14,21,22] To estimate the pure error, five center points were included. All the critical factors (bead amount, homogenization time, and lipid concentration) had three levels, which were chosen based on previous experiments. The corresponding responses (particle size/Z-Average and PDI) were determined using dynamic light scattering. Subsequently, the results were fitted to a quadratic-order model, which is mathematically described as follows:

$$Y = \propto_0 + \propto_1 A + \propto_2 B + \propto_3 C + \propto_4 AB + \propto_5 AC \\ + \propto_6 BC + \propto_7 A^2 + \propto_8 B^2 + \propto_9 C^2$$

where in this study Y = particle size/Z-Average or PDI, A = bead amount, B = lipid concentration, C = homogenization time and α = linear, interaction or quadratic regression coefficient.

For statistical validity the data of the particle size (Z-Average) model were transformed. To further improve the regression model, a model reduction was performed by excluding insignificant terms (p-value > 0.1). The model was evaluated based on the results of the analysis of variance (ANOVA), where a p-value of <0.05 was considered significant. The optimization of both responses while maintaining the desired targets of the critical factors was realized using the desirability function of the Design-Expert® software.

2.1.5. LNP characteristics measurements

2.1.5.1. Particle size, size distribution and zeta potential. Particle size, size distribution, and zeta potential were determined using a Zetasizer Nano ZS Malvern Analytics (Kassel, Germany). For measurements, 10 μl of sample was diluted in approximately 1 ml of SH buffer. Particle size measurements were performed at a backscatter angle of 173°, with three measurements per sample, each consisting of 10 runs and an equilibration time of 60 s at 25 °C. Buffer parameters were set to a viscosity of 1.1793 cP and a refractive index of 1.3437. Particle sizes are displayed as the harmonic intensity-averaged particle diameter (Z-Average) and size distribution as the polydispersity index (PDI).

For zeta potential measurements, a similar dilution was used, and analyses were carried out using a Dip Cell (Malvern Analytics, Kassel, Germany).

2.1.5.2. Encapsulation efficiency. The encapsulation efficiency was determined using the Quant-iT RiboGreen Assay (Thermo Fisher Scientific GmbH, Dreieich, Germany) according to the manufacturer's protocol for high range assays. Black 96-well plates (Greiner bio-one, Frickenhausen, Germany) were used. LNPs containing RNA were diluted with TE buffer (10 mM Tris-HCl, 1 mM EDTA, pH 7.5) to a final nucleic acid concentration of 800 ng mL^{-1}. Each sample was tested in triplicates in the presence or absence of 0.05% (v/v) Ecosurf (Carl

Roth GmbH + Co KG). Fluorescence measurements were performed using the fluorescence plate reader FLx800 (BioTek, Vermont, USA) at an emission wavelength of 528 nm and an excitation wavelength of 485 nm. Quantification of the encapsulated RNA was determined in regards on the fluorescence intensity (FI) of the non-encapsulated RNA to the FI of total miRNA content.

2.1.5.3. pH measurements. The pH of empty LNP dispersions was measured using the FiveEasy™ F20 pH meter (Mettler-Toledo GmbH, Gießen, Germany) in combination with the pH sensor InLab® Micro (Mettler-Toledo GmbH) after dilution 1 : 3.5 (V/V) with deionized water.

2.1.5.4. Cryogenic transmission electron microscopy (cryo-TEM) imaging of LNPs. miRNA LNPs for cryo-TEM imaging were prepared in water at concentration of 20 mg mL^{-1}. Subsequently, 3 µL of the sample were deposited on a Quantifoil S 7/2 copper grid (Quantifoil, Jena, Germany) that was glow discharged immediately prior to use by the PELCO easiGlow (Ted Pella, Redding, California, USA). Blotting was then performed using a Vitrobot MK IV (ThermoFisher, Waltham, Massachusetts, USA) with the following parameters: blotting time of 3 s, blot force of 8, drain time of 2 s, chamber temperature of 20 °C, relative chamber humidity of 100%, and plunge vitrification of the samples. The grids were stored in liquid nitrogen until imaging. A FEI Talos L120C at 120 kV operating voltage equipped with a Ceta 16-megapixel camera (ThermoFisher) was used for imaging.

2.1.5.5. Agarose gel for mRNA integrity investigations. For integrity measurements a 1% agarose gel was prepared using an Agarose HR-PLUS from Carl Roth GmbH + Co KG. For gel casting 5 mL of 10x MOPS buffer (0.4 M MOPS from Thermo Fisher Scientific GmbH, sodium acetate 0.1 M from Thermo Fisher Scientific GmbH, EDTA 0.01 M from Carl Roth GmbH + Co KG), 36 mL RNase free water, 9 mL 37% formaldehyde (Thermo Fisher Scientific GmbH), and 1 µL of SYBR™ Gold (Thermo Fisher Scientific GmbH) were added to 500 mg of agarose. The gel was run with 1× MOPS buffer and 110 V for 60 min using a Biometra Power Pack Modell 250 from Analytik Jena GmbH + Co. KG (Jena, Germany) utilized a PerfectBlue™ Gelsystem Mini chamber (VWR International GmbH, Darmstadt, Germany). Samples were prepared as previously described, with the exception that a 0.09 M TRIS solution (Thermo Fisher Scientific GmbH) at a pH of 9 was used to achieve deprotonation of all lipids. LNPs were purified in a similar manner as described by Packer *et al.*[23] For visualization, a Fusion FX7 (VilbertLourmat, Eberhardzell, Germany) was utilized.

2.2. Cell culture

2.2.1. Materials for cell culture. Cell experiments were conducted as previously described.[19] Knockdown efficiency was determined in HEK293A cells stable transfected with *Zoanthus* sp. green fluorescent protein (ZsGreen) from the BIOSS Centre for Biological Signalling Studies (Freiburg, Germany). Because of an overlapping emission spectrum, a non-fluorescent HEK293A cell line also from the BIOSS Centre for Biological

Signalling Studies was used for cytotoxicity assays. The cells were cultured at 37 °C and 5% CO$_2$ in Dulbecco's Modified Eagle Medium (DMEM) obtained from PAN-Biotech GmbH (Aidenbach, Germany), supplemented with 10% fetal calf serum (Sigma-Aldrich, St. Louis, USA) and 0.1% sodium pyruvate (PAN-Biotech GmbH, Aidenbach, Germany). HeLa cells from the Leibniz Institute DSMZ-German Collection of Microorganisms and Cell Cultures GmbH (Braunschweig, Germany) were used for mRNA expression and cultivated similar to the HEK293A cells.

Cells with passage numbers between 3 and 20 were used. Mycoplasma testing was performed after thawing and additionally at random time points using the MycoStrip® – Mycoplasma Detection Kit (InvivoGen Europe, Toulouse, France).

2.2.2. *In vitro* experiments

2.2.2.1. In vitro treatment of cells using miRNA-LNPs. HEK293A *Zs*Green or HEK 293A cells were seeded at 2×10^4 per well into a 24 – well plate (TPP Techno Plastic Products AG, Trasadingen, Switzerland) 24 h prior to transfection. The cells were treated in triplicates with miRNA-LNPs at a concentration of 75 nM encapsulated miRNA. Therefore, 50 µL of each miRNA-LNP dispersion, diluted in SH buffer to the desired concentration, was added to 450 µL of fresh medium. As a positive control for knockdown experiments, miRNA was transfected using Lipofectamine RNAiMAX (Thermo Fisher Scientific GmbH), and pure medium was used as a negative control. The medium containing miRNA-LNPs was replaced with 1 mL of fresh medium after 2 h, followed by incubation for 72 h until flow cytometry measurements.

2.2.2.2. Knockdown measurements. The treated cells were detached by 200 µL Accutase® (PAN-Biotech GmbH, Aidenbach, Germany) for 5 min after aspiration of the medium. Next, 800 µL medium was added to stop the enzymatic reaction. Detached cells were disaggregated and collected in precooled flow cytometry vials, followed by centrifugation at 241 rcf for 4 min at 4 °C using an Eppendorf AG Centrifuge 5804 R. The supernatants were discarded, and the resulting cell pellets were washed with phosphate buffered saline (PBS) (PAN-Biotech GmbH). A second centrifugation and washing step was performed, followed by adding 200 µL of PBS and vortexing. The cell suspensions were analyzed using a BD LSRFortessa™ flow cytometer (BD Bioscience Heidelberg, Germany). For each sample, 10 000 cell events were recorded. A 530/30 bandpass filter was used for fluorescence intensity measurements. The gating strategy is exemplary displayed in the SI section.

2.2.2.3. GFP expression of mRNA loaded LNPs in HeLa cells. HeLa cells were treated as described before by Ruppl *et al.*[24] Briefly HeLa cells were seeded in 24-well plates (60 000 cells per well) 24 h before transfection. LNPs were diluted with SH buffer and then added to achieve a final mRNA concentration of 0.5 µg mL^{-1} per well (50 µl LNP dispersion, 450 µl medium). Pure medium (DMEM, 10% fetal calf serum, 0.1% sodium pyruvate) served as the negative control. After 24 h, cells were detached and washed in a similar manner as for the

knockdown experiments. Cells were then analyzed (10 000 cell events with a 530/30 bandpass filter) by flow cytometry (BD LSRFortessa™ flow cytometer, BD Bioscience) using the BD FACSDiva™ software. The gating strategy is exemplary displayed in the SI section.

2.2.2.4. Cytotoxicity measurements. HEK293A cells were seeded, treated, and incubated in a similar manner as for the knockdown experiments. After 72 h, the cells were evaluated regarding viability, apoptosis, and necrosis using the CellEvent™ Caspase-3/7 Green Flow Cytometry Assay. Following detachment and washing, cells were stained under light-protected conditions for 30 min with 100 µl of diluted CellEvent™ Caspase-3/7 Green Detection Reagent to stain apoptotic cells. During the last five minutes, 100 µl of diluted SYTOX® AADvanced Dead Cell Stain was added to detect necrotic cells. The cells were then analyzed with a BD LSRFortessa™ cytometer (BD Biosciences) using a 530/30 nm bandpass filter for the CellEvent™ Caspase-3/7 Green Detection Reagent and a 670/30 nm bandpass filter for the SYTOX® AADvanced Dead Cell Stain, recording 10 000 events per sample. Data processing and gating were performed with BD FACSDiva™ software, with gating strategies provided in the SI.

3. Results

3.1. Downscaling in-vial homogenization

The recently published protocol for preparing LNPs with 10 mg batch sizes was systematically varied in terms of the following variables: vial type (0.5, 1.5, and 2 mL screw-cap vials), bead diameter (0.35, 0.9, and 1.5 mm), bead quantity (60 to 600 mg), and the volume of added buffer, which determines the lipid concentration during the in-vial homogenization process.[19,20] Due to economic considerations, an EPC3/Chol 55 : 45 (mol/mol) model lipid mixture was utilized. The liposomes were evaluated according to particle sizes and size distributions (PDI values) (SI, Fig. S1 and S2).

The findings confirmed the suitability of the combination of 20% lipid concentration, 2 mL vials and beads with a diameter of 1.5 mm over the full range of added beads (Fig. 1).

3.2. Optimization of the downscaled protocol using a DoE approach

The process of small-batch in-vial homogenization was refined using a DoE approach. The DoE approach was based on 2 mL vials and 1.5 mm beads and was used to investigate the effects of bead amount, lipid concentration, and homogenization time on the particle sizes (*Z*-Average) and size distributions (PDI) more precisely. A three-factor Box–Behnken design was applied with five center points. The factor settings and corresponding responses of the DoE approach are presented in the SI section (Table S1).

The regression model was evaluated using ANOVA after removing insignificant terms. To ensure statistical validity, response 1 (*Z*-Average) was transformed. The adjusted R^2 values for particle size (0.96) and PDI (0.94) were satisfactory
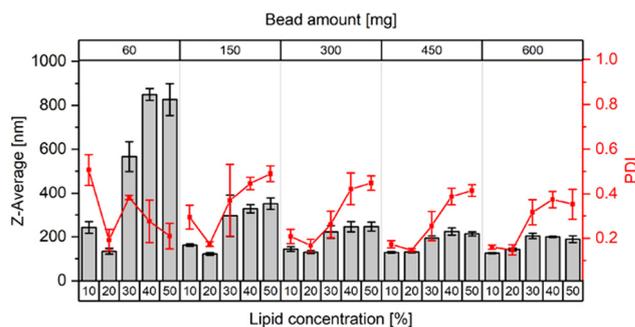

Fig. 1 Particle size (*Z*-Average) and polydispersity index (PDI) of liposomal dispersion obtained by in-vial homogenization using dual centrifugation (DC) with different lipid concentrations. Samples were produced from 1 mg EPC3/Chol (55/45) (mol/mol) under the following DC-settings: 2350 rpm, 5 min, 4 °C followed by redispersion of the vesicular phospholipid gel by DC at 1500 rpm, 2 min, 4 °C. Bead size (1.5 mm) and vial size (2 mL) were kept constant. Different amounts of beads were added in each experiment. Data are presented as mean $\pm$ SD (*n* = 3).

and aligned with predicted R^2 values (difference < 0.2). Both models showed significant *F*-values/*p*-values and an insignificant lack-of-fit, confirming model validity. Remarkably, all factors demonstrated a highly significant effect ($p < 0.0001$) on both the responses (SI Table S2).

Furthermore, the influence of each factor and interaction was examined in the response to surface plots derived from the DoE analysis (Fig. 2). The results can be summarized as follows: longer homogenization times, higher amounts of beads, and increased lipid concentrations resulted in the formation of smaller particles (Fig. 2A–C). These findings were also observed for the resulting PDI values (Fig. 2D–F), although the lipid concentration appeared to have a higher impact due to interaction effects, as evidenced by the ANOVA. Overall, the lowest level of each factor had a negative impact on the results, although this could be compensated, to a certain extent, by factors at higher levels.

The final step of the DoE study was to determine the optimum factor settings using the desirability function of the Design Expert® software. The lipid concentration was set to exactly 15% and the bead amount to the target of 80 mg, as these values corresponded to the ratio of VPG/bead amount (v/w) in the previous protocol.[19] For the homogenization time and the two corresponding responses, a minimization goal was applied to create even more gentle conditions. The resultant factor settings were 15% lipid concentration, 98 mg beads and 7.5 min homogenization time. To validate this prediction, three liposomal dispersions were prepared using this optimized protocol (confirmation runs). The resulting particle size and PDI were within the prediction range of both the regression models, indicating their validity (Table 1).

3.3. Application of the optimized protocol

To generally confirm the downscaled protocol also for LNP preparations, four different miRNA-LNPs were prepared. The miRNA-LNPs were composed of DOTAP and DOPE in two
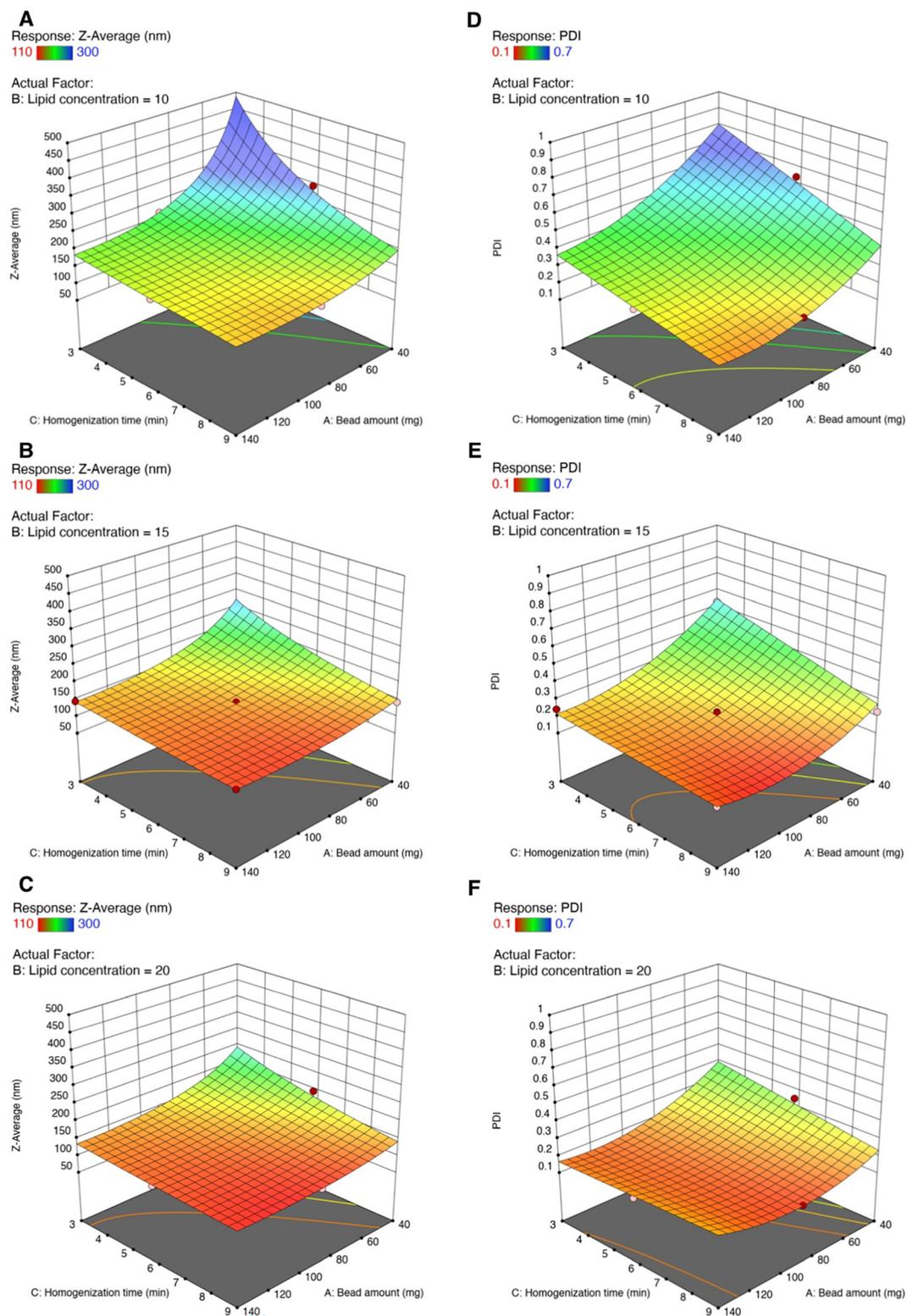
Fig. 2 Response to surface plot presenting effects of critical factors (bead amount & homogenization time) against particle size (Z-Average) (A–C) and polydispersity index (PDI) (D and E). Effects are shown for different lipid concentrations: 10% (A and D), 15% (B and E) and 20% (C and F). Spheres indicate the results of the actual experiments conducted: dark red = above surface and light red = below surface.

Table 1 Actual data mean ($n = 3$) of particle size (Z-Average) and polydispersity index (PDI) of liposomal dispersion in comparison to 95% prediction interval calculated by Design Expert® software. Samples were prepared according to optimized settings of bead amount (98 mg) and homogenization time (7.5 min) for 15% lipid concentration

Analysis	95% prediction interval low	Actual data mean	95% prediction interval high
Z-Average [nm]	118.3	132.6	133.1
PDI	0.093	0.175	0.203

different molar ratios, combined with 40 mol% cholesterol and 2 mol% of either DMPE-PEG$_{2000}$ or DMG-PEG$_{2000}$. The LNPs produced by the new protocol exhibited comparable particle sizes, PDI values, and encapsulation efficiencies as achieved in a previous study using larger batch sizes.[19] Moreover, all LNPs exhibited equivalent high knockdown efficiencies and showed either equivalent or enhanced performance compared to the commercial transfection reagent, RNAiMAX (Fig. 3).

3.4. Preparation and screening of ionizable miRNA-LNPs

3.4.1. HCl addition during lipid film preparation. The protonation step was conducted during the lipid film preparation to avoid the addition of highly concentrated acidic buffers for protonation of the ionizable lipids during the VPG preparation process. HCl was added to the organic lipid solution during the lipid film formation stage (1, 5, and 10 μmol). After diluting the VPGs with water, the LNP dispersions of both lipid compositions were slightly acidic. Notably, slightly lower pH values were observed for the formulation containing 10 mol% DODMA (Table 2).

An increase in particle size was observed in both formulations with higher amounts of HCl. In general, formulations containing 10 mol% DODMA exhibited larger particle sizes and higher PDI values. As both formulations exhibited sufficient LNP properties with the addition of 1 μmol of HCl,

Table 2 Particle size (Z-Average), polydispersity index (PDI), and pH of empty LNP dispersions produced by DC with H$_2$O as the redispersion medium. Different amounts of HCl were added during the lipid film preparation. Lipid compositions are presented as mol%. Data are derived from $n = 1$

Lipid composition of empty LNPs	n (HCl) [μmol]	pH	Z-Average [nm]	PDI
DODMA/CHOL/DSPC/ DMG-PEG$_{2000}$ (10/40/48/2)	1	2.90	152	0.208
	5	2.80	203	0.289
	10	2.75	247	0.479
DODMA/CHOL/DSPC/ DMG-PEG$_{2000}$ (50/40/8/2)	1	3.59	123	0.158
	5	3.15	135	0.119
	10	2.90	192	0.090

and to further reduce acidic exposure during lipid film preparation, this amount was selected for the subsequent experiments. The dilution of the VPGs with SH buffer for neutralization resulted in particles with an increased size (>200 nm) and PDI values (>0.35). In contrast, the dilution of the VPGs with small volumes of pure water, followed by a final dilution with concentrated SH buffer, resulted in reduced particle sizes and sufficient size distributions (Table 3).

Table 3 Particle size (Z-Average) and polydispersity index (PDI) of miRNA-LNP dispersions produced according to the new DC-protocol adjusted for ionizable LNPs, including the third step, *i.e.* dilution with concentrated SH buffer. 1 μmol of HCl was added during lipid film preparation. Lipid compositions are presented as mol%. Data are shown as the mean ± SD ($n = 3$)

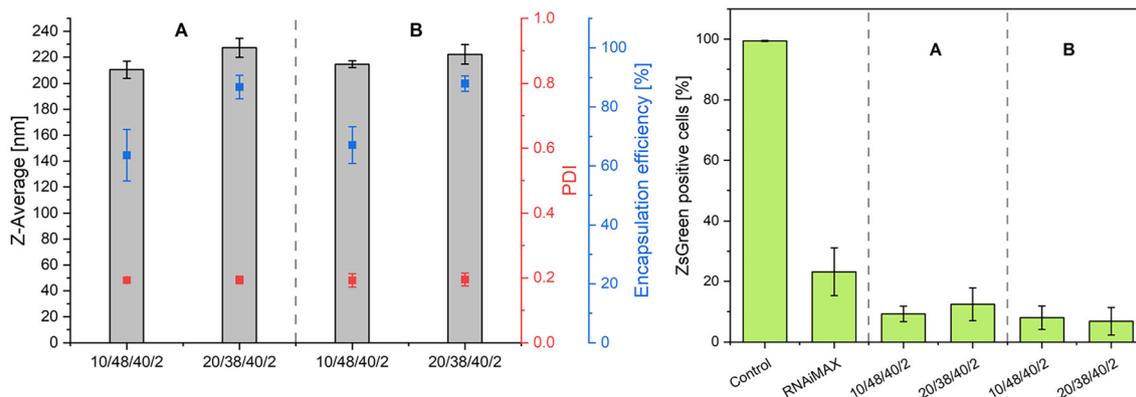| Lipid composition of miRNA-LNPs	n (HCl) [μmol]	Z-Average [nm]	PDI
DODMA/CHOL/DSPC/ DMG-PEG$_{2000}$ (10/40/48/2)	1	158.9 ± 8.6	0.169 ± 0.022
DODMA/CHOL/DSPC/ DMG-PEG$_{2000}$ (50/40/8/2)	1	147.9 ± 2.8	0.133 ± 0.012

Fig. 3 (A) DOTAP/DOPE/CHOL/DMPE-PEG$_{2000}$ (B) DOTAP/DOPE/CHOL/DMG-PEG$_{2000}$. Particle size (Z-Average), polydispersity index (PDI), and encapsulation efficiency of cationic miRNA-LNPs produced according to optimized DC protocol. Lipid compositions are presented as mol%. Knockdown efficiency in ZsGreen-expressing HEK293A cells are presented as still ZsGreen positive cells. The cells were treated with 75 nM miRNA-100-5p encapsulated in cationic LNPs for 2 h, followed by 72 h of incubation prior to analysis by flow cytometry. Data are shown as mean ± SD ($n = 3$).

3.4.2. Lipid composition screening of ionizable miRNA-LNPs. Different formulations composed of the ionizable lipid DODMA, cholesterol, helper phospholipids (DSPC or DOPE), and the PEGylated lipid DMG-PEG$_{2000}$ were examined, as illustrated in Fig. 4. The content of cholesterol and PEGylated lipid was held constant, while the molar ratios of ionizable lipids (10–50 mol%) and helper phospholipids (8–48 mol%) were systematically varied. To further evaluate the applicability of our newly established method for different ionizable lipids, we implemented combinations of the ionizable lipids SM-102 or ALC-0315 and DSPC or DOPE as helper lipids, in a manner analogous to that of the DODMA-LNPs (Fig. 4).

3.4.2.1. Particle characteristics. Almost all formulations demonstrated particle sizes below 200 nm and homogeneous size distributions with PDI values of ≤0.2 (Fig. 4). Increasing amounts of ionizable lipid tended to correlate with smaller particles, a trend that was especially pronounced in the formulation containing 10 mol% ALC-0315 and DOPE as helper phospholipid (Fig. 4C). The miRNA-LNPs containing SM-102 and DOPE as helper phospholipids exhibited slightly increased PDIs compared to those containing DSPC (Fig. 4B). Overall, the most
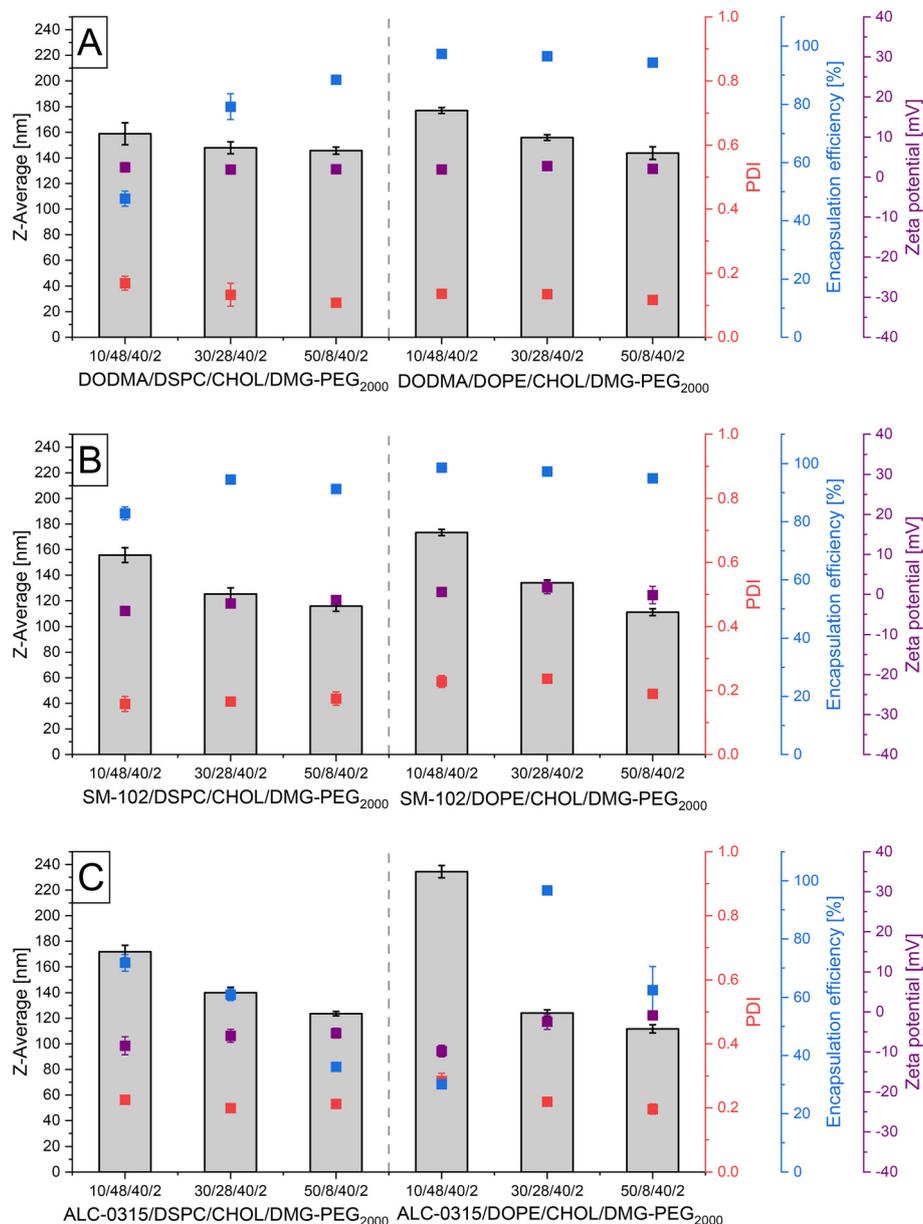

Fig. 4 Particle size (Z-Average), polydispersity index (PDI), encapsulation efficiency, and zeta potential of produced miRNA-LNPs using dual centrifugation. For each composition the molar ratio of ionizable lipid was increased while molar ratio of helper phospholipid was decreased. Each graph represents a different ionizable lipid ((A) DODMA, (B) SM-102 and (C) ALC-0315). Lipid compositions are expressed as mol%. Data are shown as mean ± SD (n = 3).

satisfactory properties in terms of particle size and size distribution were found for the formulations consisting of DODMA and the two helper phospholipids, as well as of SM-102 and DSPC (particle size ≤ 175 nm, PDI ≤ 0.175), as shown in Fig. 4.

All formulations exhibited zeta potentials in the range of −10 mV to 2.5 mV (Fig. 4) and were therefore considered to have neutral surfaces.[25] Notably, miRNA-LNPs containing ALC-0315 exhibited slightly more negative values.

3.4.2.2. Encapsulation efficiency. The highest encapsulation of miRNA of nearly 100% was detected for the formulations containing SM-102 or DODMA in combination with DOPE (Fig. 4A and B). Regarding ALC-0315 LNPs, only the formulation with 30 mol% ionizable lipid and DOPE showed comparable values (Fig. 4C). The data of miRNA-LNPs containing DODMA or SM-102 together with DSPC suggested a trend towards more sufficient encapsulation with higher content of the ionizable lipid, whereas those with ALC-0315 and DSPC showed an opposite trend (Fig. 4).

3.4.2.3. LNP morphology. Cryo-TEM images of LNPs composed of 30 or 50% of the ionizable lipid DODMA and either DSPC or DOPE as helper lipid showed non-spherical shapes with characteristic bleb structures[26,27] (Fig. 5). Sizes of the LNPs showed a reduced size in comparison to the intensity-weighted DLS data which is in accordance to published literature.[14,28] Additionally, under maximum magnification, the bleb structures manifest a heightened density, indicating they are filled with RNA.[26]

3.4.2.4. Knockdown efficiency and cytotoxicity. Numerous miRNA-LNPs successfully demonstrated sufficient knockdown of the fluorescent protein ZsGreen in the ZsGreen-expressing HEK293A cells (Fig. 6), in many cases equivalent or higher knockdown efficiencies compared to the positive control (RNAiMAX) were achieved. All miRNA-LNPs containing 30 mol% ionizable lipid and DOPE as helper phospholipid caused a nearly complete knockdown.

Notably, the miRNA-LNPs containing SM-102 or ALC-0315 displayed a different pattern than those containing DODMA. LNPs containing 30 and 50 mol% SM-102 or ALC-0315 and DSPC as helper phospholipid showed knockdown efficiencies ranging from ~70% to >85%, whereas LNPs containing 30 mol% DODMA and DSPC resulted in an insufficient knockdown (Fig. 6). In contrast to the latter, LNPs containing 30 or 50 mol% DODMA and DOPE instead of DSPC as helper phospholipid showed consistently strong knockdown efficiencies, while LNPs consisting of SM-102 or ALC-0315 (50 mol%) and DOPE exhibited only reduced knockdown efficiencies of about 50% (Fig. 6). Although some miRNA-LNPs with 10 mol% ionizable lipid achieved knockdown to a certain degree, the data suggested that a minimal molar ratio of 30% is necessary.

None of the evaluated miRNA-LNPs showed any effect on the induction of apoptosis or necrosis in HEK293A cells (SI Fig. S6).

3.4.3. Preparation of mRNA LNPs by in-vial homogenization. The most promising LNP formulations were used to prepare LNPs containing mRNA encoding for the GFP protein to analyse, whether the mRNA would withstand the in-vial homogenization process. Fig. 7 presents the size characteristics and expression efficiency of the tested samples. Sizes (Z-Average) and size distribution (PDI values) as well as encapsulation efficiencies were comparable to those of the respective miRNAs LNPs. Due to the concentration of the mRNA stock (1 mg mL^{-1}), the N/P ratios were ~29 for the LNPs containing 30% ionizable lipid, and ~50 for the LNPs containing 50% ionizable lipid. All mRNA-LNPs containing DOPE demonstrated sufficient expression of the GFP protein. Conversely, the use of DSPC as the helper lipid resulted in a complete absence of GFP expression.
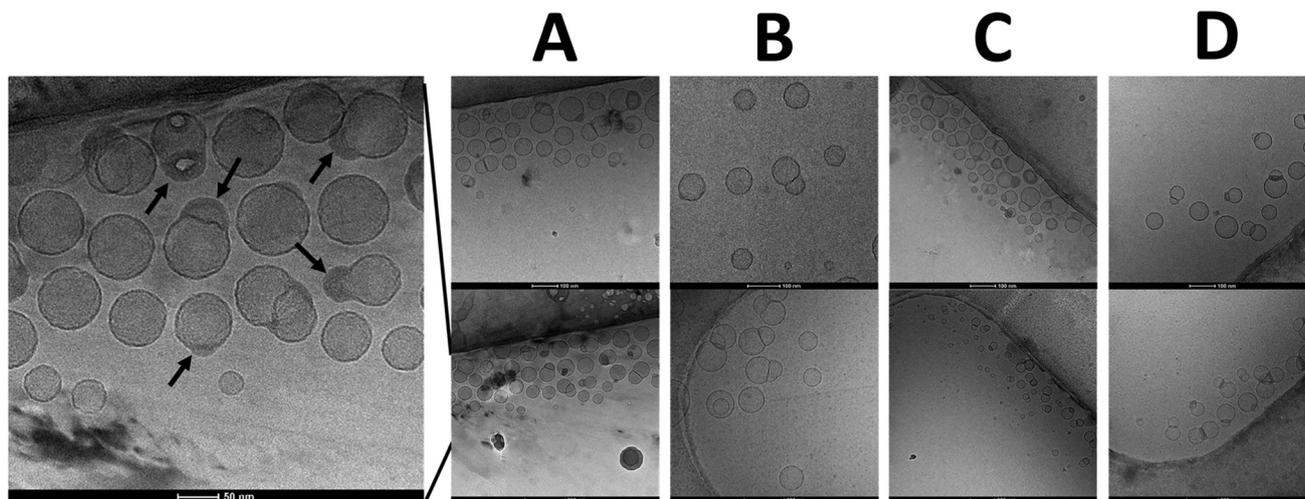

Fig. 5 LNP Morphology investigated by cryo-TEM imaging exhibits non-spherical shapes with characteristic bleb structures. Maximal magnification reveals a higher density of the blebs suggesting these structures are filled with RNA (indicated by arrows). Sizes of the LNPs are comparable lower as the measured sizes derived from DLS measurements. (A) DODMA/DSPC/CHOL/DMG-PEG$_{2000}$ (50/8/40/2); (B) DODMA/DSPC/CHOL/DMG-PEG$_{2000}$ (30/28/40/2); (C) DODMA/DOPE/CHOL/DMG-PEG$_{2000}$ (50/8/40/2); (D) DODMA/DOPE/CHOL/DMG-PEG$_{2000}$ (30/28/40/2). Lipid compositions are expressed as mol%. Scale bars represent 50 nm (left picture), 100 nm (upper row), and 200 nm (lower row).
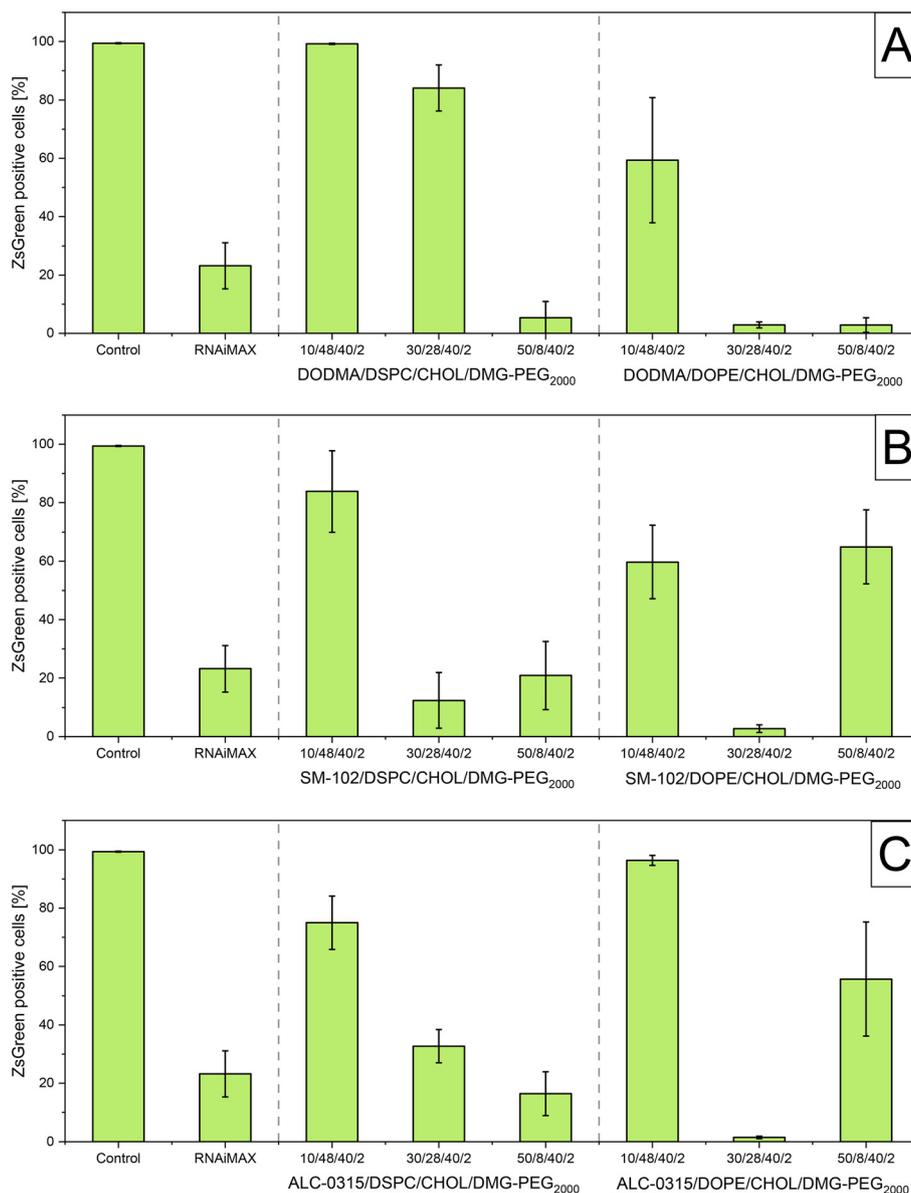
Fig. 6 Knockdown efficiency in ZsGreen-expressing HEK293A cells shown as still ZsGreen positive cells [%]. The cells were treated with 75 nM miRNA-100-5p encapsulated in ionizable LNPs for 2 h, followed by 72 h incubation prior to analysis by flow cytometry. For each composition the molar ratio of ionizable lipid was increased while molar ratio of helper phospholipid was decreased. Each graph represents a different ionizable lipid ((A) DODMA, (B) SM-102 and (C) ALC-0315). Lipid compositions are expressed as mol%. Data are shown as mean ± SD (n = 3).

Agarose gel electrophoresis was used to examine the integrity of mRNA. The GFP expression confirmed that mRNA remains intact during in-vial homogenization. However, a slight loss of mRNA integrity was observed, when mRNA underwent in-vial homogenization by DC (SI Fig. S5).

4. Discussion

4.1. Downscaling liposome and LNP preparation by DC

Reproducibility and safety are important prerequisites for economic formulation screening and development of very

small batches of liposomes and LNPs, especially when only very small amounts of active ingredient (e.g. mRNA) or lipids are available or affordable. Furthermore, only small batches are often required, e.g. for animal and cell culture experiments or in the field of patient-individualized vaccination with mRNA-loaded LNPs. LNP preparation using MMS can be carried out with very small quantities of total lipids (lower mg range). Despite this advantage, MMS is a rather complex, time consuming and expensive multistep process, which makes MMS less optimal for efficient formulation screening and development or for the patient individualized preparation of LNPs.[14,15] To combine the goal of preparing very small batches
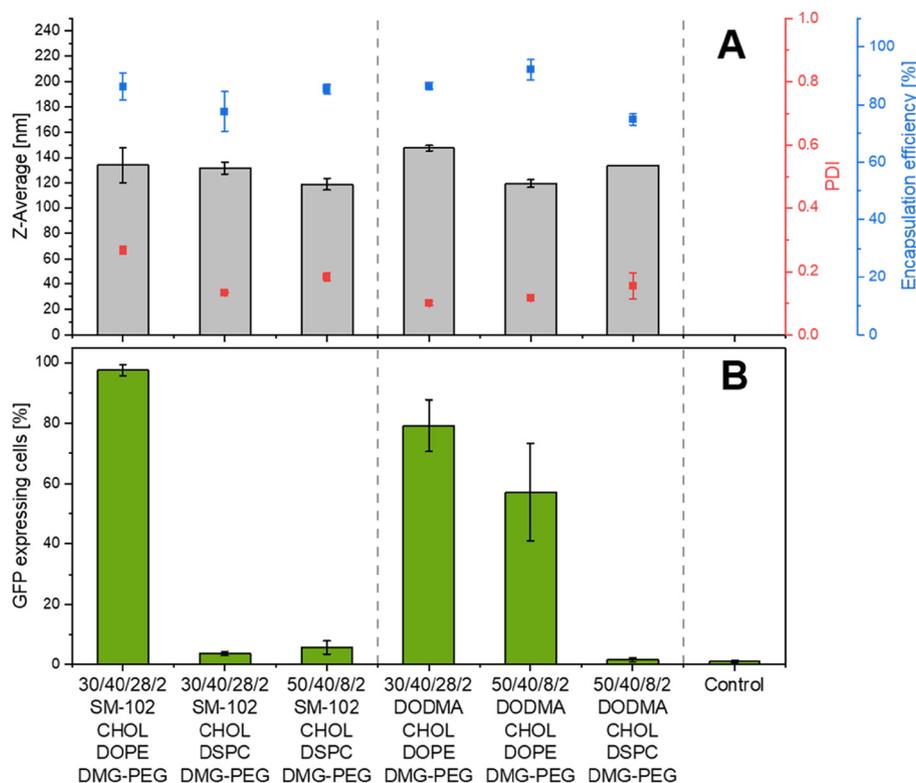
Fig. 7 (A) Particle size (*Z*-Average), polydispersity index (PDI), and encapsulation efficiency of mRNA-LNPs produced using dual centrifugation. Lipid compositions are presented as mol%. (B) Corresponding percentage of GFP expressing in HeLa cells 24 h after transfection. Data are shown as mean ± SD (*n* = 3).

of LNPs with the use of the faster and inexpensive technique of in-vial homogenization, critical steps of this newly developed LNP preparation technique have been systematically optimized for preparing very small batch sizes.

4.1.1. Bead sizes and amount. It has been reported that both, smaller bead diameters and higher bead loadings into the vial, lead to improved homogenization efficiency due to stronger bead-bead interactions during in vial homogenization.[29] Conversely, the opposite result was observed in this study using minimal lipid amounts. Given the very small batch sizes, adhesion of the primarily forming VPG to the smaller beads with its much higher surface might result in a lower percentage of VPG which is placed in the collision area of the beads. Accordingly, this effect was especially detected with the smallest beads and the highest bead loading and consequently largest bead surface (SI Fig. S2A). The use of the largest beads did not reveal any influence, which supports the hypothesis (SI Fig. S2C). Furthermore, these results indicate that the number of bead-bead interactions plays a minor role, given the advanced results obtained for larger beads. Therefore, all subsequent experiments were performed with 1.5 mm beads.

4.1.2. Vial sizes. Despite the low lipids and bead concentrations, the most effective homogenization is achieved with the largest vial (2 mL). This initially surprising result can be explained by the different lengths of the vials. In terms of effectiveness, the 2 mL and 1.5 mL vials proved to be the most

efficient (SI Fig. S1 and S2). These vials offer the longest sliding path for sample acceleration and, as a result, energy accumulation and sample friction. While the 1.5 mL and 2 mL vials have equivalent lengths, they differ in the geometry of the vial bottom. The 1.5 mL vial has a more pronounced conical shape, which can negatively impact the homogenization process, likely due to bead deflection and reduced effectiveness.

4.1.3. Lipid concentration. According to the findings of Koehler *et al.*, the lipid concentration of the VPGs significantly influences the size, size distribution, and lamellarity of the liposomes prepared by in-vial homogenization.[18,30] While the smallest liposomes were found at lipid concentrations of 15–60% when processing batches containing 100 mg of VPGs, the smallest liposomes were found in this study at lipid concentrations of 10–20% when processing only 1 mg.[18] Given the possible adhesion of water to the beads, the inner surface of the vials, and the saturation of the headspace in the vessel, the actual lipid concentration might be higher compared to that of the reported larger batch sizes. This process leads to a reduction in the water available for VPG formation, especially at very low lipid concentrations, where dead volume is particularly critical.

4.1.4. DoE-approach for protocol optimization. Given the interdependence of the parameters identified as optimizers for the initial homogenization of very small batches, it is clear that further optimization requires a multifaceted approach, as each parameter has a significant impact on all others.

Therefore, to confirm the previous results and, more importantly, to test whether individual parameters are sensitive or can be further optimized, a DoE approach was used. The DoE plots show the optimal parameters for the production of very small batches of liposomes by in-vial homogenization. They also demonstrate that these parameters are not very sensitive to minor changes (Fig. 2).

4.1.5. Preparation of cationic LNPs. The findings indicate that the application of the initial homogenization protocol to small batches, in combination with the preparation of LNPs derived from permanently cationic charged lipids, has proven to be suitable (Fig. 3). This observation underscores the conclusion that the critical parameters identified thus far for liposome preparation are of a general nature. The size and the transfection/knockdown properties of the cationic miRNA-LNPs prepared in 1 mg batches are similar to those for 10 mg batch sizes.[19] Besides batch size, the most significant differences between the different preparations were the lower N/P ratios used for the 1 mg batches. This was unavoidable because the concentration of the available miRNA solutions was fixed at that value. This finding is particularly important because it shows that the downscaled in-vial homogenization process has no negative effects on the miRNA, which again demonstrates the gentle nature of the process.

4.2. General aspects of preparation of ionizable miRNA-LNPs by in vial homogenization

To date, ionizable LNPs have typically been produced using MMS, with an acidic buffer controlling the pH of approxi-mately 4 to ensure the protonation of ionizable lipids.[11,31] Successful in-vial homogenization of lipids requires the use of highly concentrated lipid dispersions and thus very small amounts of aqueous solution. Therefore, the use of an acidic buffer with exceptionally high buffer capacity would be required.[19] Consequently, an alternative method independent of highly concentrated buffers was implemented to produce ionizable LNPs. A slight excess of HCl was added to the ethanolic lipid solution used for lipid film preparation.[19,20] This method is designed to protonate ionizable lipids. As a result, chloride salts of the ionizable lipids should be formed in the dry lipid film.[19,20] The excess gaseous HCl is subsequently removed along with the organic solvent. Protonation of lipid mixtures containing the ionizable lipid DODMA with 1 μmol of HCl resulted in functional miRNA-LNPs after in-vial homogenization, demonstrating the successful protonation of the ionizable lipids during lipid film preparation.

However, the protonation process appears to be more complex. After dilution of the LNPs with pure water, the observed pH values were lower than the pK_a value of the ionizable lipid DODMA (~7). This suggests additional protonation of the phosphodiester group of DSPC during lipid film preparation, with a pK_a of approximately 1 for the protonated DSPC.[32,33] This assumption is supported by the slightly lower pH values observed for LNP dispersions with higher molar ratios of DSPC, indicating that DSPC is at least partially protonated (Fig. 8). However, protonation of DSPC is considered advantageous as this additional proton source may help maintaining the ionized state of ionizable lipids in the aqueous dis-
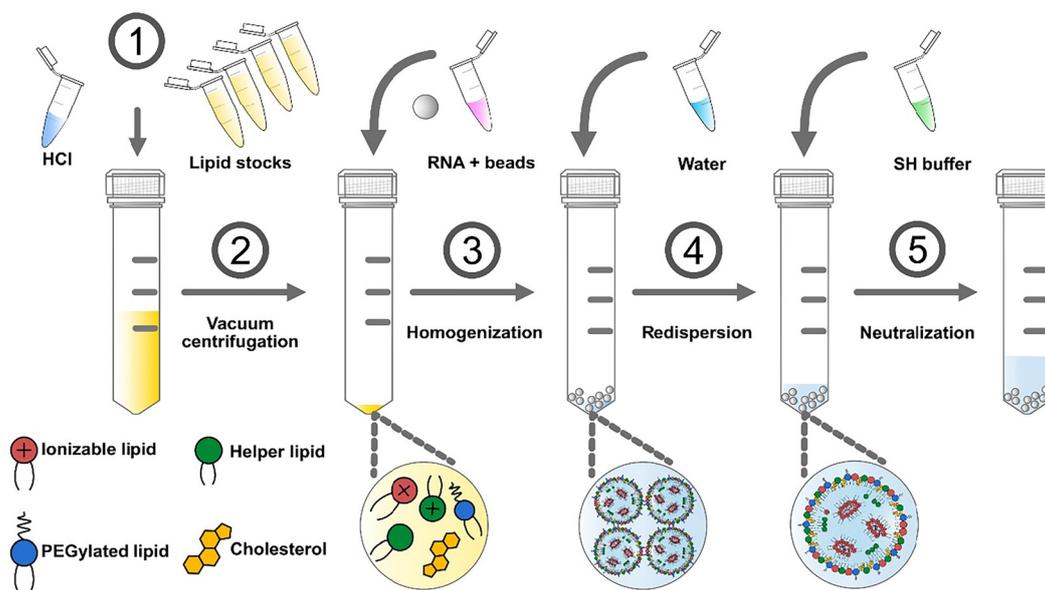

Fig. 8 Schematic illustration of the novel preparation protocol for ionizable Lipid nanoparticles (LNP) using dual centrifugation (DC). (1) Ethanolic stock solutions (~400 μL) combined with 1 μmol HCl (10 μL) in a 2 mL screwcap vial. (2) Vacuum centrifugation is employed to obtain a dry lipid film comprising ionizable lipid and helper phospholipid (at least partially) in an ionized state. (3) Following the addition of an aqueous RNA solution and beads (1.5 mm), a vesicular phospholipid gel (VPG) is generated through in-vial homogenization by DC. (4) The addition of a small amount of water for redispersion with DC at reduced speed results in the formation of a mature LNP dispersion. (5) Neutralization of the LNP dispersion is achieved by simply diluting with SH buffer.

persion during DC. It is reasonable to assume that these mechanisms are also applicable to other helper phospholipids containing a phosphodiester (*e.g.*, DOPE). Furthermore, the present study examined the influence of the pH during DC and it was demonstrated that the pH is not only crucial for the initial VPG assembly but also for the process of redispersion. The formation of a VPG in the first DC step, described as a matrix of densely packed vesicles, could possibly be compared with the formation pre-LNPs using MMS in terms of pre-vesicle formation by self-organization as described for MMS.[28]

In a previous study, Ly *et al.* demonstrated that the pH value during MMS preparation has a significant impact on the size of LNP particles.[34] The present study also revealed a relation between pH and particle size during particle formation (Table 2). It is important to note that the pH value of approximately 3 was observed for the final diluted LNP dispersions, which implies a considerably lower pH value in the first DC step than that employed in MMS.

In addition to the postulated influence of pH on the formation of pre-LNPs during in vial homogenization, a strongly negative effect on LNP properties was observed when the redispersion and neutralization using an SH-buffer of the initially formed VPGs was performed in a single step, implicating pH-dependent morphological changes. As postulated by Terada *et al.* pH neutralization (*i.e.*, dialysis) performed after MMS preparation of pre-LNPs promotes a shear stress-sensitive LNP metamorphosis, leading to an increase in particle size.[14] The present results support the hypothesis that the (pre)-LNPs in the VPG may undergo similar morphological changes due to the induced shear stress sensitivity during the neutralization process. Accordingly, the moderate shear stress involved in redispersion by DC and the LNP metamorphosis by neutralization were separated into two separate steps, as shown in Fig. 8, to overcome undesirable fusion events. First, the VPG was redispersed with pure water, allowing the pre-LNPs to mature into the final LNPs without significantly changing the pH. This approach reduces the particle sensitivity to shear stress. In the next step, the still acidic dispersion was neutralized by adding a neutral buffer without further inducing shear stress. Nevertheless, there may be differences in the maturation process of the pre-LNPs between the two preparation techniques, since unlike the DC-based approach, the pre-LNP dispersions after MMS contain ethanol, which may influence the pre-LNP maturation process (mainly fusion).[14] Nevertheless, cryo-TEM pictures show the formation of the desired bleb structures also in the LNPs produced by in-vial homogenization and thus provide first evidence to support the hypothesis (Fig. 5).[26]

4.3. Lipid composition screening of ionizable LNPs

4.3.1. miRNA loaded LNPs. An initial small batch LNP formulation screening using different ionizable lipids (DODMA, SM-102, ALC-0315) for the encapsulation and transfection of miRNA was performed. Since this RNA type has been found to be very robust, any differences in transfection behavior can thus be attributed to the new LNP preparation technique or to

the lipid composition.[35] Although the molar ratio of PEGylated lipids in the lipid mixture – a crucial factor for particle size[11] – was kept constant throughout the screening approach, a moderate variation in particle size was observed in response to a change in the molar ratio of ionizable lipids and helper lipids (DOPE, DSPC). This finding is consistent with those reported in the literature.[34] The RNA-encapsulation efficiencies of LNPs with SM-102 or DODMA are comparable to those reported for a similar N/P ratio of 6 utilized in the COVID-19 vaccines.[7] In contrast, LNPs with ALC-0315 showed a lower encapsulation and knockdown efficiency, possibly due to the lower $pK_a \sim 6$, and thus, a possibly different response to the added HCl during lipid film or the new preparation protocol established with DODMA ($pK_a \sim 7$).[36,37] Recently, an interaction effect between the molar ratio of ionizable lipids and the pH during LNP preparation using MMS on encapsulation efficiency was reported, supporting the aforementioned assumption.[34]

While LNPs with SM-102, ALC-0315, or DODMA showed comparable sizes and size distributions in this study, their knockdown efficiencies varied considerably. These differences may be partly attributed to structural differences in the ionizable lipids. Branch-ended ionizable lipids such as SM-102 or ALC-0315 have been reported to demonstrate a superior intracellular delivery of their nucleic acid cargo in comparison to two-tailed ionizable lipids like DODMA.[38,39] This is consistent with the finding that LNPs with a lower molar ratio (10–30%) of DODMA and DSPC as helper phospholipid showed reduced or almost no knockdown compared to those with SM-102, ALC-0315, and DSPC.

In contrast, LNPs with DOPE as helper phospholipid behave differently. It is generally accepted that DOPE, due to its cone-shaped structure, promotes the transition into an inverted hexagonal (H_{ii}) lipid phase during endosomal escape. This, in turn, enhances intracellular delivery and thus knockdown.[11,34] Although these effects have been observed with LNPs containing DODMA, the lower knockdown efficiency of LNPs containing 50 mol% branched-tailed ionizable lipids and DOPE as the helper phospholipid, compared to LNPs with DSPC, is contradictory. One possible reason for this phenomenon is the more rigid nature of the saturated and branched ALC-0315 and SM-102 compared to DODMA,[40] which may lead to morphological changes, resulting in an altered intracellular delivery. A recent study showed that the presence of H_{ii} lipid phases consisting of DOPE and an unsaturated two-tailed ionizable lipid in LNPs increases intracellular delivery.[41] Replacing the ionizable lipid with a saturated, more rigid analogue resulted in altered morphology and reduced intracellular delivery.

While the majority of LNP formulation studies emphasize the need for a minimum molar ratio of 40–50% ionizable lipid,[42] our study proves that a complete knockdown can be achieved with only 30% of ionizable lipid.

4.3.2. mRNA loaded LNPs. mRNA-LNPs prepared by the new technology exhibited similar sizes and size distributions to miRNA-LNPs. Only a slight decrease in encapsulation efficiency was observed, most likely due to higher N/P rations

than usual.[7] As previously stated, the elevated N/P ratios can be attributed to the minimal volumes of aqueous mRNA solution necessary for initial homogenization and the maximum mRNA concentrations that were available. According to the literature, the N/P ratios used have a significant impact on the LNP properties, including size and encapsulation efficiency.[28,43,44] Therefore, increased N/P ratios are believed to also affect the encapsulation efficiency, as demonstrated by the experimental results. Furthermore, the N/P ratio has been shown to influence transfection efficiency.[45]

In this study, GFP expression was detected exclusively in cells transfected with mRNA-LNPs using DOPE as the helper phospholipid. This finding is particularly noteworthy because one of the formulations that did not show GFP expression in the cells is almost identical to the original Spikevax® vaccine (SM-102/DSPC/CHOL/DMG-PEG$_{2000}$ 50/38.5/10/1.5). *Vice versa* this LNPs showed good transfection efficiency on the same cell line when being prepared by a T-mixing technology but with a lower N/P ratio of 6.[24] This further supports our hypothesis of a correlation between N/P ratio, lipid composition, and the resulting transfection efficiency. Another explanation for the lack of transfection of the nearly Spikevax® analogue could be mechanical stress during the LNP-preparation by in-vial homogenization, which could compromise mRNA stability when the more rigid helper phospholipid DSPC is part of the formulation. However, agarose gel electrophoresis showed virtually no loss of mRNA integrity, demonstrating that mechanical stress during in-vial homogenization had no effect on the mRNA (SI Fig. S5). Furthermore, our initial results demonstrate that fragile mRNA can be processed by in-vial homogenization with DC. This advance, which is both economical and practical, has the potential to significantly expand the applications of mRNA by addressing critical concerns regarding its production and storage stability.

5. Conclusion

This study presents a novel in-vial homogenization approach for the production of LNPs and liposomes, based on DC. The method offers notable advantages in formulation speed, process reproducibility, and resource efficiency. The successful miniaturization of the DC-based in-vial homogenization process has enabled the production of batch sizes down to 1 mg. This scale is comparable to the minimum feasible batch size achievable *via* MMS, thus offering a promising alternative for early-phase development. The new protocol ensures the production of sterile and ready-to-use LNP dispersions, while eliminating the need for acidic buffers, ethanol during production, post-preparation treatments (*e.g.* dialysis), and the use of costly materials such as microfluidic mixing devices. The system enables parallel production of up to 40 vials per run after lipid film preparation, with a formulation time of less than 10 minutes. This high-throughput capability significantly accelerates screening workflows, supporting rapid and efficient evaluation of LNP formulations.

Therefore, the approach is tailored to the needs of preclinical development.

Conflicts of interest

There are no conflicts to declare.

Data availability

The data supporting this article have been included as part of the supplementary information (SI). SI is available. The SI provides additional details on the DoE experiments, as well as the gating strategies used for the flow cytometry measurements. It also includes the agarose gel, cytotoxicity measurements, and enlarged cryo-TEM images. Further data that support the findings of this study are available from the corresponding author upon reasonable request. See DOI: https://doi.org/10.1039/d5pm00287g.

Acknowledgements

References

1 H. Iwakawa and Y. Tomari, *Mol. Cell*, 2022, **82**, 30–43.
2 M. A. Valencia-Sanchez, J. Liu, G. J. Hannon and R. Parker, *Genes Dev.*, 2006, **20**, 515–524.
3 D. P. Bartel, *Cell*, 2004, **116**, 281–297.
4 F. C. Moraes, C. Pichon, D. Letourneur and F. Chaubet, *Pharmaceutics*, 2021, **13**, 1901.
5 I. Dasgupta and A. Chatterjee, *Methods Protoc.*, 2021, **4**, 10.
6 A. A. Seyhan, *Int. J. Mol. Sci.*, 2024, **25**, 1469.
7 L. Schoenmaker, D. Witzigmann, J. A. Kulkarni, R. Verbeke, G. Kersten, W. Jiskoot and D. J. A. Crommelin, *Int. J. Pharm.*, 2021, **601**, 120586.
8 Y. Zhu, L. Zhu, X. Wang and H. Jin, *Cell Death Dis.*, 2022, **13**, 644.
9 S. F. Dowdy, *Nat. Biotechnol.*, 2017, **35**, 222–229.
10 A. Akinc, M. A. Maier, M. Manoharan, K. Fitzgerald, M. Jayaraman, S. Barros, S. Ansell, X. Du, M. J. Hope, T. D. Madden, B. L. Mui, S. C. Semple, Y. K. Tam, M. Ciufolini, D. Witzigmann, J. A. Kulkarni, R. van der Meel and P. R. Cullis, *Nat. Nanotechnol.*, 2019, **14**, 1084–1087.

11 C. Hald Albertsen, J. A. Kulkarni, D. Witzigmann, M. Lind, K. Petersson and J. B. Simonsen, *Adv. Drug Delivery Rev.*, 2022, **188**, 114416.

12 A. Vogelaar, S. Marcotte, J. Cheng, B. Oluoch and J. Zaro, *Pharmaceutics*, 2023, **15**, 1053.

13 D. C. Jürgens, L. Deßloch, D. Porras-Gonzalez, J. Winkeljann, S. Zielinski, M. Munschauer, A. L. Hörner, G. Burgstaller, B. Winkeljann and O. M. Merkel, *OpenNano*, 2023, **12**, 100161.

14 T. Terada, J. A. Kulkarni, A. Huynh, S. Chen, R. van der Meel, Y. Y. C. Tam and P. R. Cullis, *Langmuir*, 2021, **37**, 1120–1128.

15 D. Lombardo and M. A. Kiselev, *Pharmaceutics*, 2022, **14**, 543.

16 U. Massing, S. Cicko and V. Ziroli, Dual asymmetric centrifugation (DAC)–a new technique for liposome preparation, *J. Controlled Release*, 2008, **125**, 16–24.

17 J. K. Koehler, S. Schmager, V. Bender, D. Steiner and U. Massing, *Pharmaceutical*, 2023, **16**, 1519.

18 J. K. Koehler, J. Schnur, H. Heerklotz and U. Massing, *Pharmaceutics*, 2021, **13**, 2046.

19 V. Bender, C. Smolka, F. Pankratz, M. Köll-Weber, U. Massing and R. Süss, *Eur. J. Pharm. Sci.*, 2025, **208**, 107056.

20 V. Bender, L. Fuchs and R. Süss, *Int. J. Pharm.:X*, 2024, **7**, 100255.

21 R. Rampado and D. Peer, *J. Controlled Release*, 2023, **358**, 398–419.

22 G. E. P. Box and D. W. Behnken, *Technometrics*, 1960, **2**, 455–475.

23 M. Packer, D. Gyawali, R. Yerabolu, J. Schariter and P. White, *Nat. Commun.*, 2021, **12**, 6777.

24 A. Ruppl, D. Kiesewetter, M. Köll-Weber, T. Lemazurier, R. Süss and A. Allmendinger, *Int. J. Pharm.*, 2025, **671**, 125272.

25 M. C. Smith, R. M. Crist, J. D. Clogston and S. E. McNeil, *Anal. Bioanal. Chem.*, 2017, **409**, 5779–5787.

26 M. H. Y. Cheng, J. Leung, Y. Zhang, C. Strong, G. Basha, A. Momeni, Y. Chen, E. Jan, A. Abdolahzadeh, X. Wang, J. A. Kulkarni, D. Witzigmann and P. R. Cullis, *Adv. Mater.*, 2023, **35**, 2303370.

27 J. B. Simonsen, *J. Controlled Release*, 2024, **373**, 952–961.

28 J. A. Kulkarni, M. M. Darjuan, J. E. Mercer, S. Chen, R. van der Meel, J. L. Thewalt, Y. Y. C. Tam and P. R. Cullis, *ACS Nano*, 2018, **12**, 4787–4795.

29 U. Massing, S. G. Ingebrigtsen, N. Škalko-Basnet and A. M. Holsæter, in *Liposomes*, ed. A. Catala, InTech, 2017.

30 J. K. Koehler, L. Gedda, L. Wurster, J. Schnur, K. Edwards, H. Heerklotz and U. Massing, *Pharmaceutics*, 2023, **15**, 706.

31 P. R. Cullis and P. L. Felgner, *Nat. Rev. Drug Discovery*, 2024, **23**, 709–722.

32 M. R. Moncelli, L. Becucci and R. Guidelli, *Biophys. J.*, 1994, **66**, 1969–1980.

33 D. Marsh, *Handbook of Lipid Bilayers*, CRC Press, 2nd edn, 2013.

34 H. H. Ly, S. Daniel, S. K. V. Soriano, Z. Kis and A. K. Blakney, *Mol. Pharm.*, 2022, **19**, 1892–1905.

35 M. Hirsch, V. Ziroli, M. Helm and U. Massing, *J. Controlled Release*, 2009, **135**, 80–88.

36 P. Patel, N. M. Ibrahim and K. Cheng, *Trends Pharmacol. Sci.*, 2021, **42**, 448–460.

37 S. Patel, R. C. Ryals, K. K. Weller, M. E. Pennesi and G. Sahay, *J. Controlled Release*, 2019, **303**, 91–100.

38 X. Han, H. Zhang, K. Butowska, K. L. Swingle, M.-G. Alameh, D. Weissman and M. J. Mitchell, *Nat. Commun.*, 2021, **12**, 7233.

39 F. Ferraresso, A. W. Strilchuk, L. J. Juang, L. G. Poole, J. P. Luyendyk and C. J. Kastrup, *Mol. Pharm.*, 2022, **19**, 2175–2182.

40 G. B. Schober, S. Story and D. P. Arya, *Sci. Rep.*, 2024, **14**, 2403.

41 R. Pattipeiluhu, Y. Zeng, M. M. R. M. Hendrix, I. K. Voets, A. Kros and T. H. Sharp, *Nat. Commun.*, 2024, **15**, 1303.

42 S. H. El Moukhtari, E. Garbayo, A. Amundarain, S. Pascual-Gil, A. Carrasco-León, F. Prosper, X. Agirre and M. J. Blanco-Prieto, *J. Controlled Release*, 2023, **361**, 130–146.

43 H. Seo, L. Jeon, J. Kwon and H. Lee, *Adv. Healthcare Mater.*, 2023, **12**, 2203033.

44 J. A. Kulkarni, J. L. Myhre, S. Chen, Y. Y. C. Tam, A. Danescu, J. M. Richman and P. R. Cullis, *Nanomedicine*, 2017, **13**, 1377–1387.

45 M. A. Haque, A. Shrestha, C. M. Mikelis and G. Mattheolabakis, *Int. J. Pharm.:X*, 2024, **8**, 100283.